METEOROLOGY AND OCEANOGRAPHY. June 6–10. 1994, Monterey, CA.
Published by the American Meteorological Society, Boston. MA.

6.1

SSM/I RAINFALL VOLUME CORRELATED WITH DEEPENING RATE IN EXTRATROPICAL CYCLONES

Grant W. Petty*
Douglas K. Miller

Purdue University
West Lafayette, Indiana

1 INTRODUCTION

Identifying systematic physical differences in the development of cyclones with ordinary and explosive deepening rates — the latter nicknamed "bombs" – has been the focus of much research activity in the past decade. It has generally been concluded that no process is by itself sufficient for explosive cyclone development, rather the synergy of several physical processes leads to cases of rapid development (Uccellini et al. 1987).

Our ability to make a diagnosis and prognosis of the essential physics is limited by our ability to make high quality observations of the necessary parameters. The majority of explosively deepening cyclones occur in marine environments (Roebber 1989), regions where meteorological observations are sparse. For this reason, much interest has recently been devoted to identifying "signatures" of rapid cyclogenesis in images obtained by satellite instruments. Success in discovering explosive cyclone signatures would have tremendous value as a nowcasting tool.

One proposed approach has been to look at regions of upper level divergence using cloud drift winds (Ellrod 1986) observed by infrared or visible waveband instruments. The difficulty in applying this method is that high level clouds can obscure important information at slightly lower levels.

A different method involves using images of upper-tropospheric warm anomalies observed by a microwave sounder (e.g. MSU) in conjunction with models, analysis tools, and other observations to identify the existence of favorable conditions for intense cyclone development (Velden 1992).

A final approach is to examine various moisture parameters observed by satellite instruments. Microwave instruments such as the Special Sensor Microwave/Imager (SSM/I) have the ability to give vertically integrated moisture information even in the presence of dense cloud cover. Recent research has focused on the comparison of water vapor fields in rapid and non-rapid cases of cyclogenesis (McMurdie 1989).

With the emergence of reasonably robust, physically based rain rate algorithms designed for the SSM/I, a unique opportunity exists to directly observe a physical component which can contribute to or be a signature of cyclone deepening (latent heat release). The emphasis of the research in this paper is to seek systematic differences in rain rate observed by the SSM/I, using the algorithm of Petty (1994), in cases of explosive and nonexplosive cyclone deepening.

2 METHODOLOGY

The cyclones included in this study occurred in the extratropical regions of the North Pacific and Atlantic Oceans during the period from September 1987 through April 1988 and had complete SSM/I coverage within a 250 km radius of the low center. The final storm sample consisted of 31 SSM/I overpasses of 23 intensifying cyclones whose deepening rates ranged from 3.5 mb/(12 h) to 31.0 mb/(12 h). Cyclones of all intensity classes were included.

Central pressures and deepening rates of the chosen cases were computed for the time of the SSM/I overpass using European Centre for Medium-Range Weather Forecasts (ECMWF) gridded 12 hour analyses. Cyclone central pressures at non-synoptic times which corresponded to the time of the SSM/I overpass were computed assuming a constant deepening rate. Cyclone positions were determined subjectively using SSM/I imagery.

The strength of cyclone development had to be defined in a quantitative manner to allow correlation with SSM/I precipitation observations. The most frequently used method to characterize cyclone development is related to the deepening rate of the central pressure at the surface. Sanders and Gyakum (1980) proposed that a cyclone be classified as a

*Corresponding Author Address: Grant W. Petty, Purdue Univ., Earth and Atmospheric Sciences Dept., West Lafayette, IN, 47907-1397

Table 1. Correlation of rain volume amount (for pixels whose rain rate exceeds 7 mm/h) to various measures of cyclone intensity or intensification.

PARAMETER	CORR. COEFF.
central pressure	-0.42
deepening rate	-0.74
absolute normalized deepening rate	0.80

rapid deepener if its deepening rate met or exceeded the threshold of 24 mb $(24\ \mathrm{h})^{-1}$. A more stringent threshold was used in the Experiment on Rapidly Intensifying Cyclones over the Atlantic (ERICA) which was a deepening rate of 10 mb or greater in a 6 h period (Reed 1993).

Three measures of cyclone intensity or intensification were correlated with several different parameters related to SSM/I observations of rain rate. These measures were surface central pressure, surface central pressure deepening rate, and absolute normalized surface central pressure deepening rate. The latter is defined as

$$ANDR = \frac{DR}{THRES.} \quad (1)$$

$$THRES. = \frac{10\ \mathrm{mb}}{6\ \mathrm{h}} \cdot \frac{\sin(\Phi)}{\sin(60)} \quad (2)$$

where Φ is the latitude of the cyclone at the time of the SSM/I overpass and DR is the surface central pressure deepening rate.

The different computed parameters based on SSM/I observations of rain rate for the correlations were rain area, rain area where rain rate exceeds a given threshold, rain volume (area of a given SSM/I pixel multiplied by its rain rate), and rain volume where rain rate exceeds a given threshold. Only those pixels in the northern half of each cyclone were used for the computations so that precipitation associated with the dynamics in the vicinity of the storm center could be separated from precipitation associated with cold frontal dynamics.

3 RESULTS

Correlations between SSM/I rain volume where rain rate exceeds 7 mm h^{-1} and the three tested measures of cyclone intensity or intensification are shown in Table 1. Cyclone unnormalized deepening rate DR and absolute normalized deepening rate $ANDR$ give remarkably high correlation coefficients

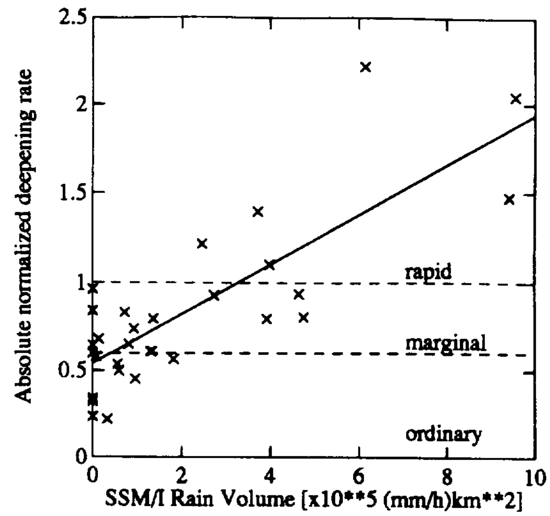

Fig. 1: SSM/I-observed rain volume (for pixels whose rain rate exceeds 7 mm h^{-1}) plotted against $ANDR$.

of −0.74 and 0.80, respectively, when related to SSM/I observations of precipitation. The major difference between the two intensification parameters is that $ANDR$ takes into account the latitudinal dependence of the Coriolis effect which makes it easier for cyclones to attain a large deepening rate the closer its position to the poles.

Cyclone surface central pressure consistently gave the poorest correlation to the tested SSM/I-based rain rate parameters. This might be expected since a cyclone can attain a low central pressure and remain unexceptional in terms of its associated dynamical forcing when a cyclone is advected into a region of low "background" pressure (frequently observed in the vicinity of Greenland).

The relationship between the $ANDR$ parameter and the total rain volume where rain rate exceeds 7 mm h^{-1} for the 31 SSM/I overpasses is shown in figure 1. This combination of cyclone intensification and SSM/I precipitation parameters gave the best correlation for the given storm sample. The solid line represents the best fit line using least squares regression. The upper dashed line is the threshold for a period of deepening to be classified as rapid or as marginal. The lower dashed line is the threshold for a period of deepening to be categorized as marginal or as ordinary. Eight cyclones have two coincident SSM/I overpasses while fifteen cyclones only have one coincident SSM/I overpass.

The storm sample is such that 6 periods of deepening are categorized as rapid, 16 periods of deepening are categorized as marginal and 9 periods are classified as ordinary.

For the 6 rapid data points, none has a thresholded rain volume amount falling below $2 \cdot 10^5$ mm h^{-1} km^2. For those points categorized as ordinary, none has a thresholded rain volume amount that exceeds $2 \cdot 10^5$ mm h^{-1} km^2. There are 8 points that have a non-zero $ANDR$ value, yet have zero rain volume amounts. These points represent overpasses where no SSM/I pixel retrieved a rain rate amount of at least 7 mm h^{-1} in the northern half of the cyclone.

An SSM/I-observed rain rate of 7 mm h^{-1} represents an intense precipitation event most likely associated with convection. The high correlation between rain volume for SSM/I pixels exceeding this rain rate and $ANDR$ seems to suggest that the convective component of precipitation in a storm is most directly related to the processes involved in its intensification.

Of the 8 points having non-zero $ANDR$ amounts with zero rain volume, 5 fall into the marginal deepening category. There are several possible explanations for this apparent inconsistency with the above conclusion. First, the ECMWF surface pressure analyses have a time resolution of 12 h. It is possible that at the time of an SSM/I overpass a cyclone may have been actually weakening rather than intensifying as shown in the ECMWF analyses. Second, it was stated above that no physical process is by itself sufficient for cyclone intensification. The 5 marginal/zero rain volume cases may represent cyclones where "dry" physics processes (vorticity and/or temperature advections) are the dominant factors in determining intensification. Finally, all 5 cases had a non-zero stable precipitation component. In these cases it may be that latent heat release from the stable precipitation was enough to increase intensification so that the period of deepening was categorized as marginal.

4 FUTURE WORK

The significant issue needing resolution is whether the latent heating associated with intense precipitation processes is *causing* additional deepening of cyclones pushing them to the "rapid" category or, rather, the intense precipitation processes are the *result of* vigorous secondary circulations caused by a storm environment being significantly out of some balanced state. The authors hope to use a RISC workstation version of the Penn State Mesoscale Model Version 4 (MM4) in conjunction with the SSM/I imagery of the 31 overpasses to address this question. Model output will also help to explain the above noted inconsistency in the 5 cyclone periods where there is marginal deepening and zero rain volume for pixels whose rain rate exceeds 7 mm h^{-1}.

Acknowledgments

This work was supported by NASA Grant NAG 8-918. Also, D. Miller was supported by a NASA Graduate Student Researchers Program Fellowship (NGT-51077). The authors wish to thank Dr. Lynn McMurdie for her assistance with data collection and for helpful discussions.

REFERENCES

Ellrod, G., 1986: Deepening rate of extratropical cyclones estimated from divergence of upper level cloud drift winds. Preprints of the Second Conference on Satellite Meteorology/Remote Sensing and Applications, 13–16 May, Williamsburg, VA., *American Meteorological Society,* 197–201

McMurdie, L.A., 1989: Interpretation of integrated water vapor patterns in oceanic midlatitude cyclones derived from the Scanning Multichannel Microwave Radiometer. Ph.D. dissertation, Dept. of Atmospheric Sciences, University of Washington, 223pp.

Petty, G.W., 1994: Physical retrievals of over-ocean rain rate from multichannel microwave imagery. Part II: Algorithm implementation. In press, *Meteorol. Atmos. Phys.*

Reed, R.J., G.A. Grell, and Y.H. Kuo, 1993: The ERICA IOP 5 storm. Part I: analysis and simulation. *Mon. Wea. Rev.,* **121,** 1577–1594

Roebber, P.J., 1989: On the statistical analysis of cyclone deepening rates. *Mon. Wea. Rev.,* **117,** 2293–2298

Sanders, F., and J.R. Gyakum, 1980: Synoptic-dynamic climatology of the "bomb". *Mon. Wea. Rev.,* **108,** 1589–1606

Uccellini, L.W., R.A. Petersen, K.F. Brill, P.J. Kocin, and J.J. Tuccillo, 1987: Synergistic interactions between an upper-level jet streak and diabatic processes that influence the development of a low-level jet and a secondary coastal cyclone. *Mon. Wea. Rev.,* **115,** 2227–2261

Velden, C.S., 1992: Satellite-based microwave observations of tropopause-level thermal anomalies: Qualitative applications in extratropical cyclone events. *Wea. Forecasting,* **7,** 669–682